Collegiate Aviation Review International

Volume 41 | Issue 1 Peer Reviewed Article #9

7-8-2023

Pilot's Guide to Maximum Glide Performance: Optimum Bank Angles in Gliding Turns

Nate Callender
Middle Tennessee State University

A pilot's awareness of an airplane's power-off glide performance is critical for successfully responding to an engine failure in flight. Pilot's operating handbooks (POH) and airplane flight manuals (AFM) provide the minimum required glide information; however, there is more information that can better equip pilots to extract the maximum glide performance from an airplane. Information about the effect of weight changes on the glide is available but does not seem to be common knowledge among pilots. Information concerning optimum bank angles to use in gliding turns is much less available and seems completely unknown to pilots. This paper provides guidance to pilots for applying weight correction to the best glide speed. It also presents a methodology for determining the optimum bank angle in power-off glides that require a gliding turn to a safe landing location. The results of the study include the optimum gliding bank angles for airplanes with varying glide ratios (GR) along with rules of thumb for determining the optimum bank angle in flight. The findings of this research can be utilized to supplement 1) the glide performance information used and presented by digital avionics, 2) the glide information contained in POHs and AFMs, and 3) flight training for power-off glides with or without turns to safe landing locations, all with the goal of providing pilots with more tools to land safely at a suitable location in the event of an engine failure.

Recommended Citation:
Callender, N. (2023). Pilot's guide to maximum glide performance: Optimum bank angles in gliding turns. *Collegiate Aviation Review International*, 41(1), 180-208. Retrieved from https://ojs.library.okstate.edu/osu/index.php/CARI/article/view/9516/8477

A publication of the University Aviation Association, © 2023, ISSN: 1523-5955

Introduction

Power-off glide performance is a consideration that all pilots should have prior to and during every flight, especially when in a single-engine airplane. As with other airplane performance information, an airplane's glide performance is presented in the pilot's operating handbook (POH) and/or the airplane flight manual (AFM). That is, of course, if the airplane was certified after 1996. In February of that year, the Federal Aviation Administration (FAA) mandated that POHs and/or AFMs include a minimum of 1) the airplane's maximum horizontal distance covered over the ground per $1{,}000\ ft$ of altitude lost in a power-off glide and 2) the airspeed required when doing so (Glide: Single-Engine Airplanes, 1996).

While these pieces of performance information are valuable in planning and performing a power-off glide, there is more information that pilots can know about optimizing an airplane's power-off glide performance. Commonly used publications and handbooks such as the FAA's Airplane Flying Handbook (2021) and the well-known text Aerodynamics for Naval Aviators (Hurt, 1965) include aerodynamic information and practical instructions regarding glide performance. These and other pilot-focused texts clearly present the two required glide performance values (or their equivalent) required by the FAA. They go further by indicating that the airspeed necessary for maximum glide performance is a function of weight. Chapter 3 of the Airplane Flying Handbook (2021) states that a weight adjustment is required; however, it does not present a method for making the adjustment. Hurt (1965) refers to the weight correction, and he presents an equation that can be used to make it.

Another important component of power-off glide performance is the planning for and execution of a required turn to a landing destination during the glide. When the engine failure occurs on or shortly after takeoff, the possibility of returning to the departure runway is referred to as the "impossible turn". Chapter 18 of the Airplane Flying Handbook (2021) presents general considerations for attempting such a turn, and articles, such as those by Rogers (1995) and Collazo Garcia et al. (2021), present more specific guidance to include an optimal bank angle to use in the turn.

For power-off glides being conducted from a more substantial altitude, selection of and route planning to a suitable landing location is very important. Much research has been conducted into determining optimum glide trajectories using Dubins paths to landing locations based upon terrain, winds, runway headings, airport locations, and an airplane's aerodynamic characteristics. Examples of such work are the articles by Atkins, Portillo, & Strube (2006); Chitsaz & LaValle (2007); Meuleau, Plaunt, Smith, & Smith (2009); Adler, Bar-Gill, & Shimkin (2012); Di Donato & Atkins (2016); Stephan & Fichter (2016); and Segal, Bar-Gill, & Shimkin (2019). Previous research has been focused on very specific cases, the results of which were only applicable to those cases. The research was also conducted using numerical algorithms, well

suited to computational analysis, but much less suited to practical use by pilots either in preparation for the possibility of an engine failure or during an actual power-off glide.

It is the purpose of this research to develop practical guidance for pilots to use in preparation for and in the conduct of power-off glides to safe landing locations that optimize the glide performance of the airplane. This paper intends to serve as an updated source of information and as a practical guide for glide performance. Guidance for applying the known weight correction to glide airspeed will be presented, and new research into optimal bank angles for gliding turns will be shared to include pilot rules-of-thumb for its application.

Glide Performance

Wings Level Glide

Gliding, as discussed in this paper, is considered with no power (engine-out) and in calm wind conditions. Wings-level gliding is presented first. A gliding airplane is shown in Figure 1, along with velocity and forces. Having no engine power to produce thrust, a component of the airplane's weight(W_T), is needed to overcome the airplane's drag (D), which is always directed opposite the direction of the airplane's motion or in the same direction as the relative wind (RW). The only way for this to occur is in descent. The airplane's velocity (v) is shown to be along an axis (the flight direction) at an angle (γ) below the horizon (the horizontal axis). γ is also known as the glide angle. The airplane's flight direction must be set such that its W_T is equal (and opposite) to its D in order to maintain its velocity in the flight direction. Lift (L), by definition, is perpendicular to the RW. When L is equal (and opposite) to the normal component (normal to the flight direction) of the airplane's weight (W_N), the airplane will descend at a constant γ. In short, the sum of forces in any direction is zero for a steady, unaccelerated glide.

A closer inspection can be made of the airplane's W and its components. The angle of separation between W and W_N is equivalent to the glide angle, γ, and W_N and W_T are perpendicular to one another. For right triangles such as this one, a basic trigonometric relationship relates these two components, as shown in Equation 1.

$$\tan\gamma = \frac{W_T}{W_N} \tag{1}$$

In a steady glide, D and L can then be substituted for W_T and W_N, respectively. Following these substitutions and solving for γ results in Equation 2.

$$\gamma = \tan^{-1}\left(\frac{1}{L/D}\right) \tag{2}$$

Equation 2 reveals the aerodynamic nature of glide performance.

All lifting devices, whether 2D airfoils, 3D wings, or entire aircraft, can be described by their aerodynamic characteristics. The typical presentation of these characteristics is in graphical form, with which the reader of this paper is most likely already familiar. An example of such a presentation is shown in Figure 2.

Figure 1

Free Body Diagram of an Airplane in a Power-off Glide

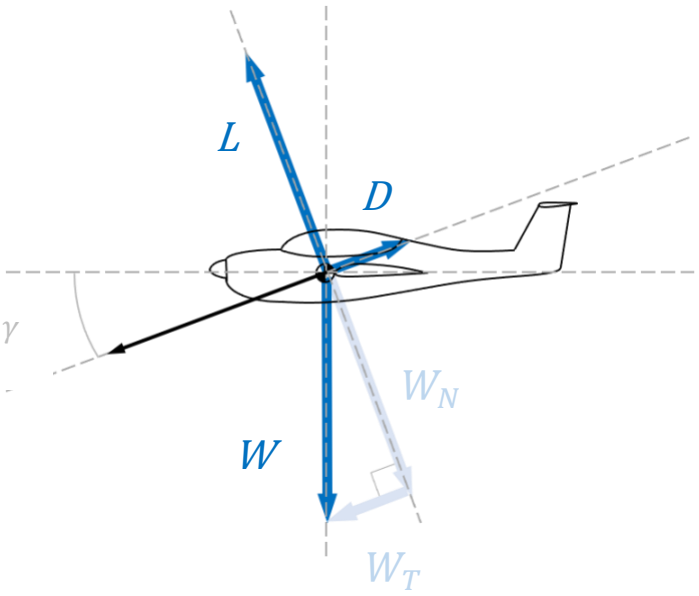

Figure 2

NACA 6612 Aerodynamic Characteristic Curves

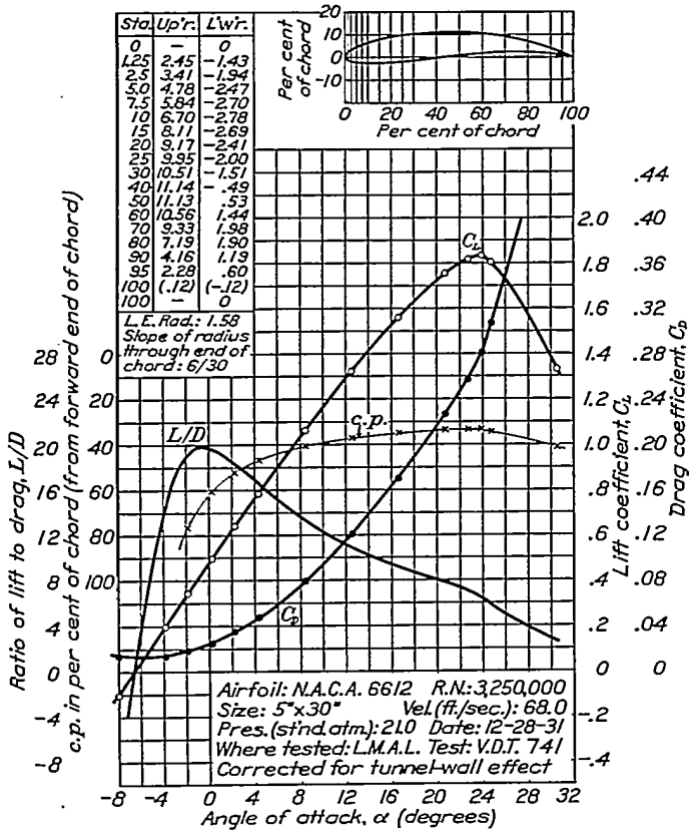

Note. Adapted from The Characteristics of 78 Related Airfoil Sections from Tests in the Variable-Density Wind Tunnel, NACA-TR-460 (1933) by Jacobs, E., Ward, K.E., & Pinkerton, R.M., retrieved from ntrs.nasa.gov.

Four basic aerodynamic characteristics are presented in Figure 2 for the NACA 6612 airfoil: the lift coefficient (C_L), the drag coefficient (C_D), the lift-to-drag ratio (L/D), and the center of pressure (CP). Each of these is a nondimensional value that represents different aspects of the airfoil's aerodynamic behavior as a function of the airfoil's angle of attack (α). C_L and C_D represent the lift and drag forces that can be created by the airfoil. The CP represents the chordwise location of those forces. The airfoil's lift will be maximized when operated at its highest lift coefficient $\left(C_{L_{max}}\right)$. The angle of attack at which this occurs is known as the critical angle of attack (α_{crit}). Maximizing the airfoil's lift is desirable for slow flight and maneuvering; however, it is accompanied by high drag, which requires high power, and is therefore not ideal for all flight conditions, especially power-off, gliding flight. Rather than taking the airfoil's C_L in isolation, comparing the C_L to the C_D at any angle of attack will provide a more complete aerodynamic picture of the airfoil's performance. This comparison was captured by L/D. The higher the L/D, the more lift an airfoil can create for a given amount of drag; or put another way, for a given amount of lift, the airfoil will produce less drag. Therefore, L/D is an indication of the airfoil's aerodynamic effectiveness (effectiveness being defined as the ability of the airfoil to produce what is desired (L) while minimizing what is not (D)). As can be seen in Figure 2, the NACA 6612's L/D curve achieves a maximum value $((L/D)_{max})$ at a specific angle of attack, known as the optimum angle of attack $\left(\alpha_{opt}\right)$.

Figure 2 presents an example of one airfoil's aerodynamic characteristics. As previously mentioned, all lifting devices, including entire airplanes, can be described by characteristics such as these; therefore, all airplanes will have an α_{opt} and an associated $(L/D)_{max}$. According to Equation 2, L/D is the only input needed to determine an airplane's glide angle. The lower the glide angle (γ), the higher an airplane's maximum glide range will be. Substituting $(L/D)_{max}$ into Equation 2 yeilds the minimum possible glide angle as shown in Equation 3.

$$\gamma_{min} = \tan^{-1}\left(\frac{1}{(L/D)_{max}}\right) \tag{3}$$

The intent of this article, as is articulated in the title, is to provide glide performance guidance to pilots. Although glide performance depends upon a specific aerodynamic characteristic, $\left(L/D\right)_{max}$, obtained when operating at a specific angle of attack, α_{opt}, that results in the lowest glide angle, γ_{min}; pilot's operating handbooks (POH) and airplane flight manuals (AFM), the primary sources of performance guidance for pilots, do not use this terminology. Recall the right triangle in Figure 2 that includes the airplane's weight, the weight's components, and the glide angle. Figure 3 presents this triangle again, with the substitutions of D and L for W_T and W_N. It also presents another triangle that represents the distance traveled in the flight direction and that distance's components in the horizontal and vertical axes. The distance traveled along the flight direction can be separated into the ground distance covered while gliding (x) and the associated altitude lost (h). These two components are at right angles to one another and can be related to one another via Equation 4.

$$\tan\gamma = \frac{h}{x} \tag{4}$$

Figure 3
Distance Travelled while Gliding

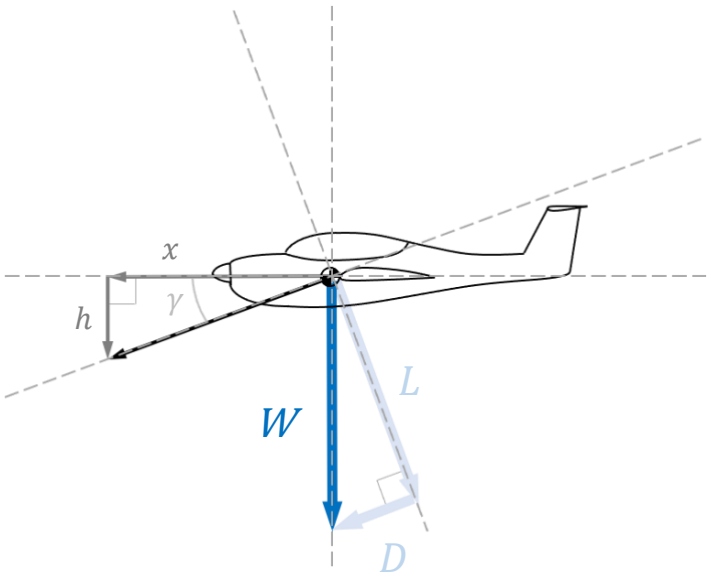

Lift and drag can also be related to one another in the same way via Equation 5.

$$\tan\gamma = \frac{D}{L} \tag{5}$$

Equations 4 and 5 can be equated and solved for x as shown in Equation 6.

$$x = h\left(\frac{L}{D}\right) \tag{6}$$

Equation 6 provides the ability to calculate the ground distance covered from a known altitude for a given L/D. Maximum glide range, R_G, is obtained from Equation 6 by substituting $(L/D)_{max}$ as shown in Equation 7.

$$R_G = h\left(\frac{L}{D}\right)_{max} \tag{7}$$

Again, $(L/D)_{max}$ does not appear in POHs or AFMs, at least not by that name. The ratio of the maximum ground distance covered for a given amount of altitude lost in a glide is defined to be glide ratio (GR). GR is therefore associated with gliding at γ_{min}. Reciprocating and equating Equations 4 and 5 while at γ_{min} reveals that an airplane's $(L/D)_{max}$ and its GR are equal. GR is typically included in POHs and AFMs as one of the primary metrics for an airplane's glide performance capability. Not all handbooks will include GR since glide performance information was not required by federal regulation until 1996. Aircraft certified prior to 1996 might include a GR, a graph of altitude vs. glide range (from which GR can be extracted), the distance traveled for $1{,}000\ ft$ of altitude lost or no glide performance at all.

Substituting GR into Equation 7 yields Equation 8, a more pilot-oriented equation for glide range.

$$R_G = h(GR) \tag{8}$$

Equation 8 can be used, with an appropriate conversion to either statute or nautical miles (assuming h is in ft), to determine possible landing locations within the airplane's glide range. In order to enable the airplane to achieve this range, a pilot needs more information. Specifically, the pilot would need to know the airplane's α_{opt}. Flying at this angle would enable the airplane to achieve its $(L/D)_{max}$ thereby minimizing its glide angle and maximizing its glide range. Flying based on angle of attack is the most effective way to maximize power-off glide range; however, civilian airplanes are not typically equipped with angle of attack indicators. Even if they were, federal regulations do not require POHs nor AFMs to contain an airplane's α_{opt}. What they are required to provide is the airspeed that enables maximum glide range, v_G. Advisory Circular AC 23-8C (2011) provides recommended techniques for flight testing Part 23 certified aircraft, including the flight test used to determine maximum glide performance. The test includes a series of power-off glides to be conducted through a range of airspeeds. An airplane's v_G can be identified from a plot of the data collected during the glides. The value is then published in the POH or AFM in several locations, most notably in the Emergency Procedures chapter. Unless a pilot has v_G memorized (which the author would recommend), the handbook's Emergency Procedure for power-off, maximum range gliding would need to be referenced (which the author also recommends) following an in-flight engine failure where the engine cannot be restarted and a power-off glide to a suitable landing site must take place.

Effect of Weight

One of the necessary conditions for presenting glide information in POHs or AFMs is that the performance information must be for the airplane at its maximum takeoff weight (MTOW). The published v_G is, therefore, accurate if and only if the airplane is at MTOW. The reality for many/most flights is that they begin with the airplane below MTOW, and even if they did begin at MTOW, the airplane's weight is always decreasing in line with its fuel flow. This means that establishing the published v_G in order to maximize the glide range will not actually maximize the glide. It will come close to doing so, but more performance is available. In order to truly obtain maximum glide performance, v_G must be adjusted for the airplane's weight at the time that power is lost. Here is that process. It begins with a conceptual scenario in which an airplane is flying straight and level at *MSL* at its *MTOW*. Let the aircraft be doing this at the published v_G with the angle of attack necessary to develop enough lift (L_i) to balance its weight. This balance is captured in the lift equation, as shown in Equation 9.

$$L_i = \frac{1}{2} C_L \rho_0 v_G^2 S = MTOW \tag{9}$$

The next step is to decrease the weight of the airplane to a new value, W_N, while maintaining altitude and angle of attack. Maintaining altitude keeps density (ρ_0) constant, and maintaining the angle of attack keeps the lift coefficient constant. In order to decrease the lift to L_N, to accommodate the new weight, the only option remaining, assuming the wing area (S) is also constant, is to decrease airspeed. Equation 10 shows this new condition.

$$L_N = \frac{1}{2} C_L \rho_0 v_{G_N}^2 S = W_N \tag{10}$$

Finally, Equation 10 is divided by Equation 9 and solved for the new airspeed, v_{G_N}, as shown in Equation 11.

$$v_{G_N} = v_G \sqrt{\frac{w_N}{MTOW}} \tag{11}$$

With two handbook values, $MTOW$ and v_G, and Equation 11, the airspeed that will actually maximize the airplane's glide range can be calculated.

The simplicity of Equation 11 makes it accessible to pilots in an engine-out scenario, especially if the aircraft is equipped with a fuel flow meter or fuel counter that keeps up with the amount of fuel used. The weight of the fuel used subtracted from the airplane's loaded weight results in the new weight, W_N. At a minimum, the author recommends calculating and knowing the lower limit of v_{G_N} for any airplane. For example, an A36 Beechcraft Bonanza has a $MTOW$ of $3{,}650\ lbs$ and a v_G of $110\ KIAS$ (2006). With no usable fuel, no passengers, and no cargo, the A36 and pilot might weigh on the order of $2{,}700\ lbs$. Using Equation 11 with these inputs results in a minimum expected value of v_{G_N} as shown in Equation 12.

$$v_{G_N} = 110 \sqrt{\frac{2{,}700}{3{,}650}} = 94.6\ KIAS \tag{12}$$

With this value for v_{G_N} and the published v_G, the lower and upper boundaries for the speed for maximum glide range for the airplane can be used for interpolation for any airplane weight. Interpolating is relatively easy; however, basic interpolations are linear, whereas the change in speed, according to Equation 11, is not. Another method would be to prepare and use a plot, as shown in example A36 in Figure 4. A pilot equipped with a plot similar to Figure 4 for any airplane could quickly and easily identify the best airspeed to fly in an engine-out situation. This type of plot could easily be created in commonly available spreadsheet software (i.e., Microsoft Excel) using Equation 11. Whether using a plot, interpolating between maximum and minimum speeds, or calculating the value directly, in order to ensure the best glide range possible, a pilot should (and is able to) adjust an airplane's maximum range glide speed for weight.

Figure 4
Speed for Maximum Glide Range vs. Weight for Example A36

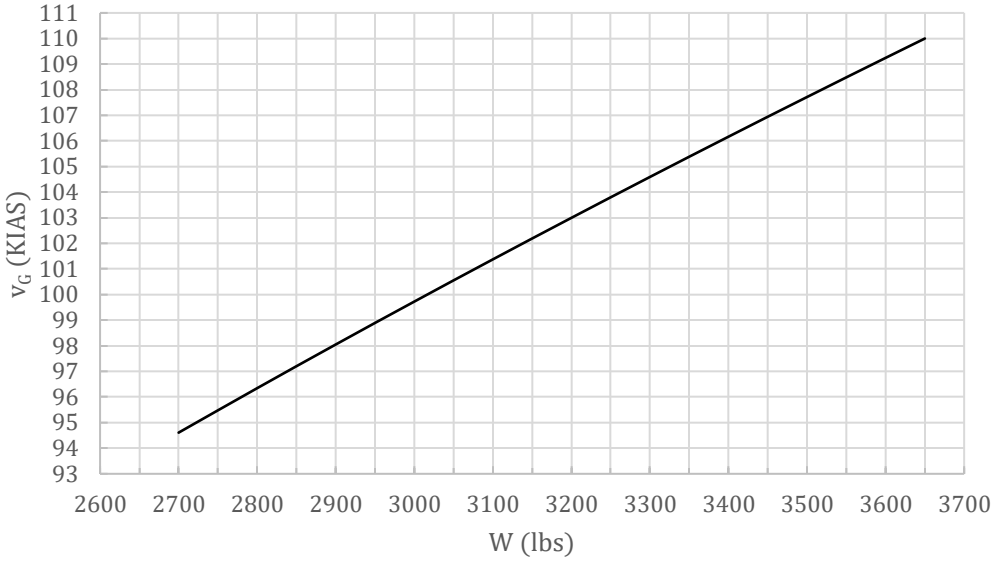

Effect of Turning

Just as glide information in airplanes' POHs and AFMs only applies to MTOW, the glide information that they present is also only for wings-level (non-turning) flights. Figure 5 presents a front view of an airplane in a banked turn.

Figure 5
Front View of Turning Airplane

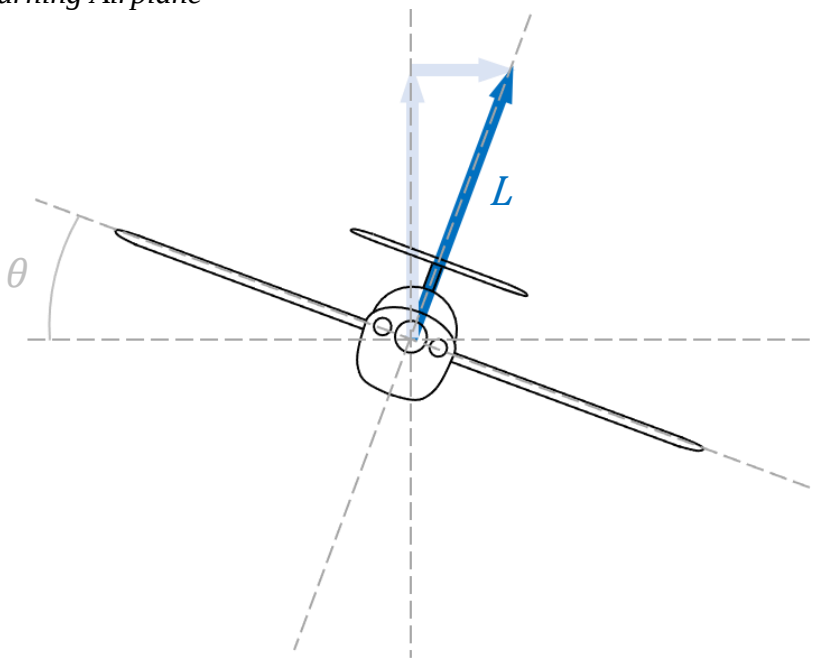

As seen in the figure, the lift is always perpendicular to the lateral axis; therefore, it will change direction in keeping with the bank angle. When the engine is operating, the bank angle would be accompanied by increased back pressure and/or increased power in order to maintain altitude in a coordinated turn. In an engine-out banked turn, maintaining altitude isn't possible, so neither increased back pressure nor increased power is useful (or even possible). Assuming that a turn is initiated at v_G, the same lift-to-drag ratio will be maintained; however, the lift will be directed as shown in Figure 5. With lift at this angle, its component in the vertical direction is reduced. The vertical component of lift is what contributes to glide performance. This is demonstrated by a reduction in GR according to Equation 13 where GR_θ represents the reduced GR in a gliding turn compared to the GR in a wings-level glide.

$$GR_\theta = GR \cos\theta \tag{13}$$

Figure 6 shows the consequence of turning at various bank angles on GR according to Equation 13. The significant effect of bank angle on GR is clear as bank angles increase. For example, an airplane in a gliding turn with $30°$ of bank will still have approximately 87% of its wings-level GR. The same airplane in a gliding turn with $60°$ of bank will only be able to produce 50% of its wings-level GR. The clear takeaway is that wings-level glides offer maximum glide range. If only the best destinations were always straight ahead in engine-out scenarios. How to deal with necessary (and suboptimal) turns to a safe landing location will be dealt with in the next section.

Figure 6
GR_θ vs. θ as a % of Wings-Level GR

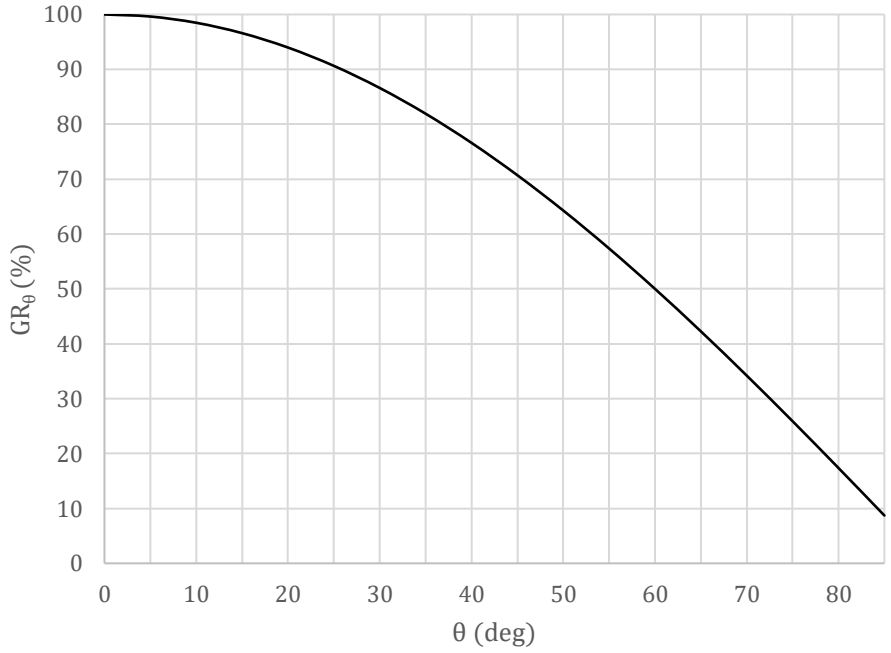

Gliding Turns to Destination

Glide Path with Required Turn

Unless an engine failure occurs within the glide range of the destination airport, which would typically be located straight ahead, a turn to an appropriate landing location will be necessary. It is clear from Equation 13 and Figure 6 that turning in a power-off glide isn't great for extending the glide range. If and when a turn is necessary, the question is how best to do it. From Equation 13, the lowest bank angle possible would be best. That is true; however, a turn's footprint as represented by the turn radius (r) must also be considered. In a constant altitude, coordinated turn, turn radius is calculated via Equation 14.

$$r = \frac{v^2}{g \tan \theta} \tag{14}$$

In a power-off glide, Equation 14 must be modified, resulting in Equation 15 (Asselin, 1997).

$$r = \frac{v^2}{g \tan \theta \cos \gamma} \tag{15}$$

The equation for glide angle (γ) is derived by rearranging Equation 5 with a substitution from Equation 13, as shown in Equation 16.

$$\gamma = \tan^{-1}\left(\frac{1}{GR \cos \theta}\right) \tag{16}$$

The results of Equations 15 and 16 can be visualized with an example. Take, for instance, an airplane gliding at $100\ KTAS$. If the airplane has a GR of 10:1, Figure 7 shows its turn radius as a function of bank angle. While a low bank angle will preserve the airplane's GR, it will result in a large turn radius. Turn radius contributes to the distance $\left(d_{\Delta\phi}\right)$ that must be covered, as viewed from above, while making a heading change $(\Delta\phi)$, as shown in Equation 17.

$$d_{\Delta\phi} = r \cdot \Delta\phi \tag{17}$$

Figure 7
Glide Ratio vs. Bank Angle for an Example Gliding Airplane

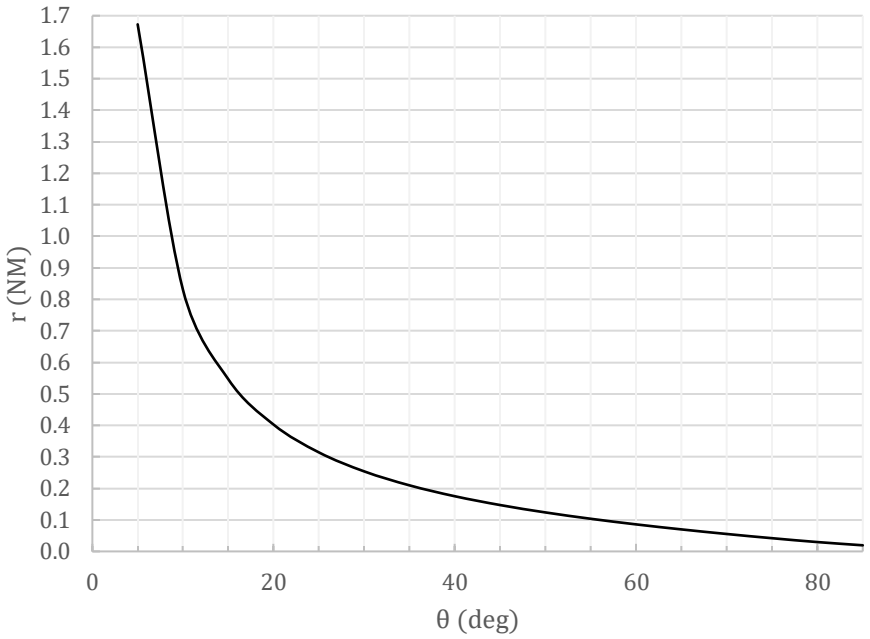

It is important to note that the heading change must be in radians in Equation 17. Continuing the example from above, let the airplane's distance covered over the ground while gliding at two bank angles ($5° \; and \; 60°$) be calculated for a $180°$ heading change. The airplane gliding with a $5°$ bank angle will cover $5.25 \; NM$ over the ground, while the airplane gliding with a $60°$ bank angle will cover only $0.27 \; NM$… almost twenty times less! The distances covered in the turn are depicted in Figure 8. Lower bank angles result in higher lift to drag ratios, GR_θ, but they also result in greater ground distances. Greater ground distances mean more altitude will be lost during the direction change. Large bank angles greatly reduce lift to drag, but they allow for direction changes with much smaller ground distances required. The bank angle that a pilot should choose in a power-off glide when a heading change is necessary is not immediately evident. It is a balancing act between preserving lift to drag ratio and minimizing the ground distance covered in the turn.

Calculating Altitude on Arrival at Destination

Calculations were conducted for an airplane with several different lift-to-drag ratios representative of a range of general aviation airplanes. The airplane's glide range was calculated from an initial altitude from which an engine failure occurred. Safe landing sites were located at bearings from $10°$ to $175°$ from the initial heading of the airplane. Glides were initiated with turns to intercept a path to the landing site. Bank angles in the turn to the intercept path were varied from $10°$ to $80°$. Figure 9 presents an example of a calculated path that would be necessary to reach a safe landing destination.

Figure 8
Distance Covered in a 180° *Turn at Two Bank Angles*

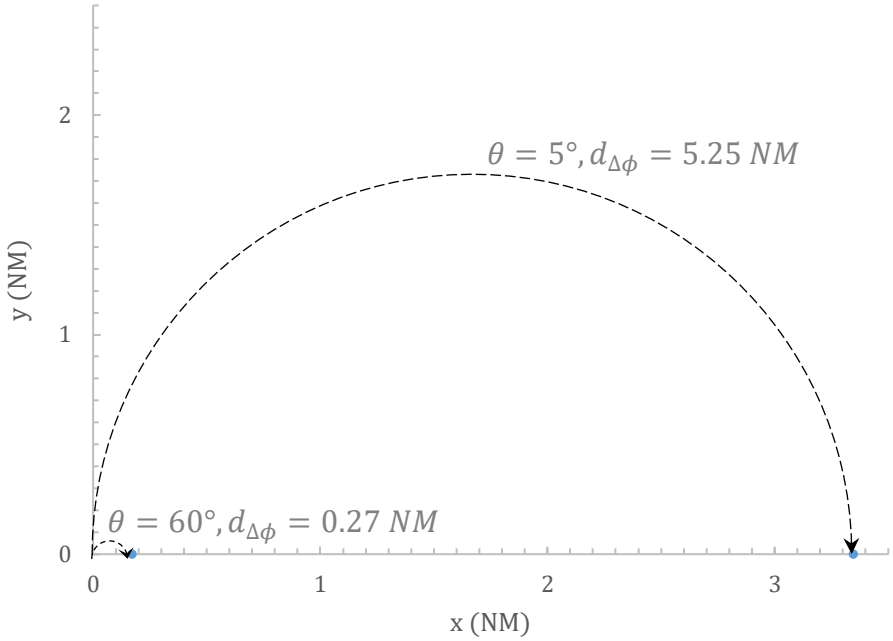

Figure 9
Glide Path to a Safe Landing Destination

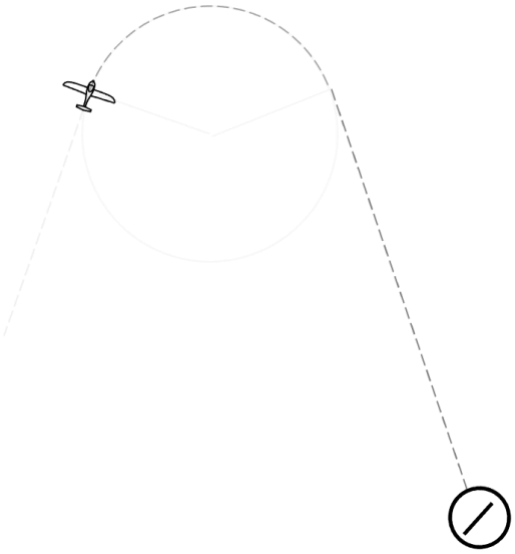

Each glide distance calculation began by setting the airplane's GR and v_G. The GR was used, along with a preselected AGL height (h), to calculate and set the distance (d) to a landing location that would allow the airplane to safely glide to the location with altitude to spare, if the landing location was on the airplane's original heading (ϕ_1). In other words, a power-off glide requiring no turn would be possible to the landing location. With the height and distance to the landing location settled, the landing location was set at the first bearing (ϕ_2), which required a

gliding turn. The scenario is shown in Figure 10, including all distances and angles used to calculate the glide range.

Figure 10
Glide Path with Distances and Angles used to Calculate Glide Range

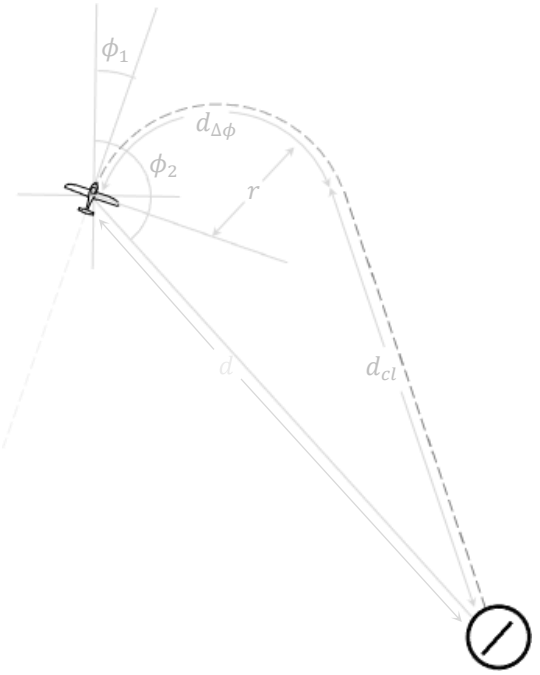

The process began with the lowest bank angle (θ). Equation 15 was then used to calculate the airplane's turn radius (r). Equations 18-23 were used to calculate the final heading (ϕ_{int}) that marked the point in the turn at which an intercept path the airport was achieved.

$$d_{cl} = \sqrt{[d \sin \phi_2 - r \sin(\phi_1 + 90)]^2 + [d \sin \phi_2 - r \cos(\phi_1 + 90)]^2} \quad (18)$$

$$\beta_1 = \sin^{-1}\left(\frac{r}{d_{cl}}\right) \quad (19)$$

$$\beta_2 = 90 - \beta_1 \quad (20)$$

$$\beta_3 = \tan^{-1}\left[\frac{d \cos \phi_2 - r \cos(\phi_1 + 90)}{d \sin \phi_2 - r \sin(\phi_1 + 90)}\right] \quad (21)$$

$$\Delta\phi = 180 - \phi_1 - \beta_2 - \beta_3 \quad (22)$$

$$\phi_{int} = \phi_1 + \Delta\phi \quad (23)$$

In these equations, d is the distance from the aircraft location to the airport; ϕ_1 is the aircraft's flight path direction; ϕ_2 is the airport direction from the aircraft position; d_{cl} is the distance to the airport after turning; β_1, β_2, and β_3 are geometric calculations used to determine the aircraft's necessary direction change $(\Delta\phi)$ and its final direction (ϕ_{int}) to the airport.

Equations 17 and 22 were then used to calculate the ground distance covered $\left(d_{\Delta\phi}\right)$ in the turn to the intercept path. The altitude lost in the turn $\left(\Delta h_{\Delta\phi}\right)$ was calculated using Equation 24, which uses GR_θ from Equation 13.

$$\Delta h_{\Delta\phi} = \frac{d_{\Delta\phi}}{GR_{\theta}} \quad (24)$$

The remaining distance to the landing site (d_{int}) on the intercept heading was then calculated using Equation 25.

$$d_{int} = \sqrt{{d_{cl}}^2 - r^2} \quad (25)$$

The altitude lost during the final glide on the intercept heading was calculated using Equation 26.

$$\Delta h_{int} = \frac{d_{int}}{GR} \quad (26)$$

The last step was to calculate the final altitude (h_f) upon arrival at the landing site using Equation 27.

$$h_f = h - \Delta h_{\Delta\phi} - \Delta h_{int} \quad (27)$$

The airplane characteristic that remained constant for all calculations was the airplane's best range glide speed: $v_G = 100\ KIAS$. This was adjusted to TAS as appropriate to the altitude for each calculation.

The first example calculations are based upon an airplane with an GR of 10. The example altitude was $6{,}000\ ft$ with a landing site $9\ NM$ away. In a straight-line glide, this airplane would be capable of gliding to a distance of $9.87\ NM$ over flat terrain. The airplane's heading (ϕ_1) for the example calculation, was $360°$, the bearing to the first landing location (ϕ_2) was set to $010°$, and the first bank angle (θ) used during the turn was $10°$. For this glide, the distance travelled while turning $(d_{\Delta\phi})$ was $0.18\ NM$. The distance traveled after the turn on the intercept course (d_{int}) was $8.83\ NM$ for a total distance (d_T) of $9.01\ NM$, and the final altitude upon arrival at the landing location (h_f) was $529\ ft$.

The scenarios evaluated were for three GRs (8, 10, and 12); four altitude and distance to the landing location combinations per GR (e.g., for $GR = 8$, $1{,}000\ ft\ AGL/1.2\ NM$; $2{,}500\ ft\ AGL/3\ NM$; $5{,}000\ ft\ AGL/6\ NM$; and $10{,}000\ ft\ AGL/12\ NM$); bearings to the landing site ranging from $10°$ to $175°$; and bank angles ranging from $10°$ to $80°$. Results for the example scenario ($GR = 10$; $6{,}000\ ft\ AGL/9\ NM$; $\phi_2 = 10°$) throughout the range of bank angles are presented in Table 1. The data shows that any bank angle from $10°$ to $80°$ would result in a similar altitude upon arrival at the destination located on a $10°$ bearing from the beginning of the glide; however, lower bank angles provided a slight advantage with the least altitude lost from a $10°$ bank angle turn.

Table 1
Glide Calculations with: $GR = 10$; $6{,}000\ ft\ AGL/9\ NM$; and $\phi_2 = 10°$

θ (°)	$d_{\Delta\phi}\ (NM)$	$\Delta h_{\Delta\phi}\ (ft)$	$d_{int}\ (NM)$	$h_f\ (ft)$
10	**0.18**	**108.0**	**8.83**	**529.4**
20	0.08	54.6	8.92	528.0
30	0.05	37.3	8.95	526.4
40	0.04	29.0	8.96	524.7
50	0.03	24.4	8.97	522.8
60	0.02	21.8	8.98	520.7
70	0.01	20.5	8.99	518.1
80	0.01	21.7	8.99	513.7

For this scenario, the lower bank angle's preservation of GR outweighed the additional travel distance required in such a shallow turn. For comparison, the data for a glide to a landing location on a bearing of $90°$ from the airplane's original heading are presented in Table 2. The glide to this landing location was also possible with a turn using any of the tested bank angles; however, the lowest bank angle was no longer ideal. The additional air distance that accompanied the lower bank angle turns resulted in more altitude lost upon arrival at the destination. The optimal bank angle appears to be very close to $50°$ in this case. Further comparison is presented using the data for a glide to a landing location on a bearing of $150°$ from the airplane's original heading, as presented in Table 3.

Table 2
Glide Calculations with: $GR = 10$; $6{,}000\ ft\ AGL/9\ NM$; and $\phi_2 = 90°$

θ (°)	$d_{\Delta\phi}\ (NM)$	$\Delta h_{\Delta\phi}\ (ft)$	$d_{int}\ (NM)$	$h_f\ (ft)$
10	1.68	1038.7	7.95	133.9
20	0.78	506.5	8.51	325.8
30	0.49	342.2	8.69	377.2
40	0.33	264.8	8.79	395.5
50	**0.23**	**222.0**	**8.85**	**400.2**
60	0.16	197.2	8.90	397.0
70	0.10	185.2	8.93	386.7
80	0.06	195.3	8.96	357.8

Table 3
Glide Calculations with: $GR = 10$; $6{,}000\ ft\ AGL/9\ NM$; and $\phi_2 = 150°$

θ (°)	$d_{\Delta\phi}\ (NM)$	$\Delta h_{\Delta\phi}\ (ft)$	$d_{int}\ (NM)$	$h_f\ (ft)$
10	2.82	1737.3	8.49	-895.2
20	1.31	846.8	8.76	-166.9
30	0.81	571.6	8.85	53.1
40	0.56	442.1	8.89	153.5
50	0.39	370.5	8.93	206.3
60	0.27	329.0	8.95	233.8
70	**0.17**	**308.9**	**8.97**	**242.8**
80	0.09	325.7	8.98	216.7

Glides to this landing location were not possible using turns at all bank angles. Although $10°$ and $20°$ banked turns preserve a higher GR, the additional flight distance required with such shallow turns resulted in excessive altitude loss and the inability to reach the landing location, as revealed by the negative final altitudes. Of the bank angles that enabled the airplane to reach its destination, the optimum bank angle for this scenario was approximately $70°$. Figure 11 presents curves of final altitude versus bank angle for each landing destination located at a different bearing from the airplane's original heading.

Optimum Bank Angles

In order to identify the optimum bank angle from each curve, second-order polynomials were fitted to the data for the three bank angles that resulted in the highest final altitudes for each glide to a specific destination, examples of which are shown in Figure 12 for final destinations located $10°$ to $90°$ from the airplane's original heading. Using the destination at $\phi_2 = 90°$ from Figure 12 as an example, its second-order polynomial curve fit resulted in Equation 28.

$$h_f = -0.0395908 \cdot \theta^2 + 4.0360093 \cdot \theta + 297.4067019 \quad (28)$$

The derivative of Equation 28 was set equal to zero and solved for θ, which revealed that the optimum bank angle for this scenario was $51°$. The process of differentiating a curve's polynomial, setting it equal to zero, and solving for the optimum bank angle was conducted for each curve. The results were then visualized, as seen in Figure 13 for the $GR = 10$*;* $6{,}000\ ft\ AGL/9\ NM$ scenario.

Figure 11

Final Altitude vs. Bank Angle for $GR = 10$; 6,000 $ft\ AGL/9\ NM$

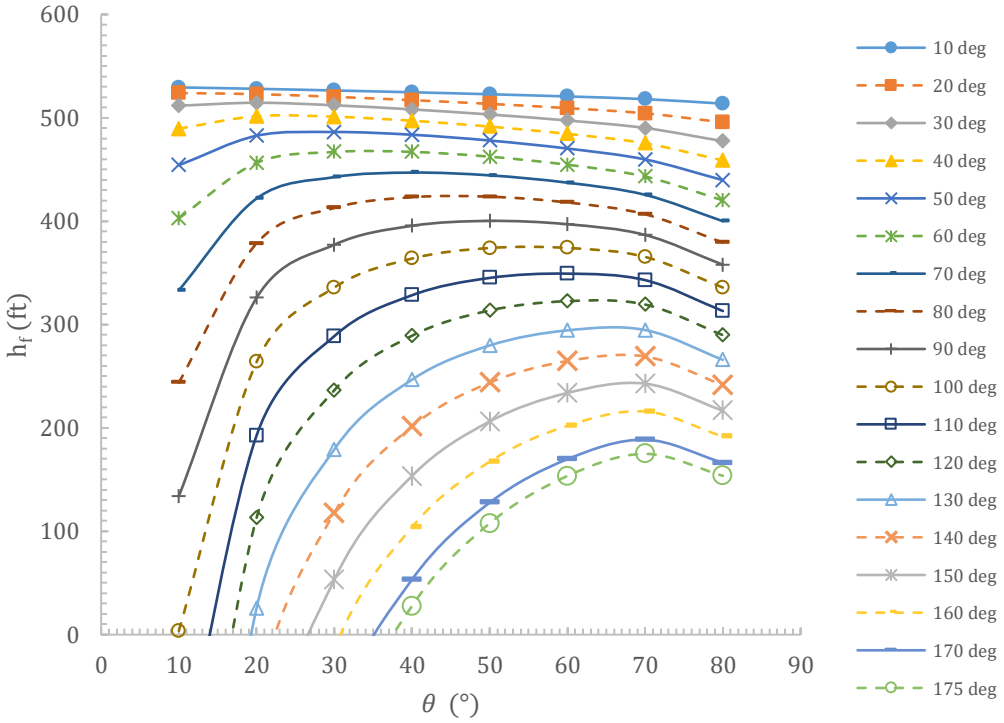

Figure 12

Final Altitude vs. Bank Angle Peaks for $GR = 10$; 6,000 $ft\ AGL/9\ NM$; and ϕ_2: $10° - 90°$

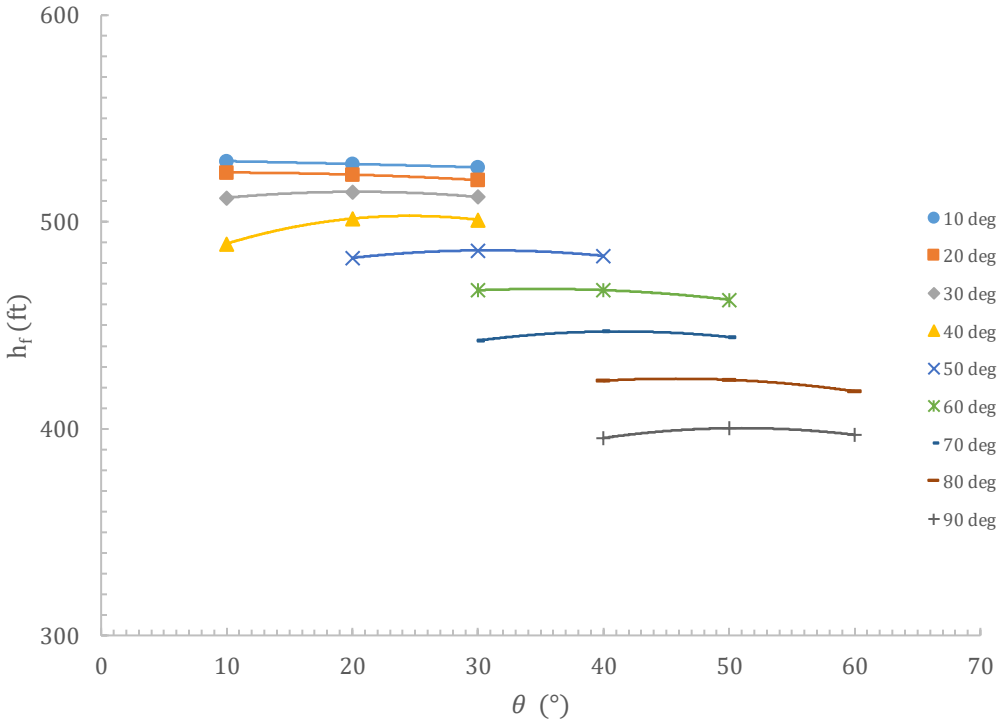

Figure 13
Optimum Bank Angle vs. Bearing to Destination for $GR = 10$; 6,000 $ft\ AGL/9\ NM$

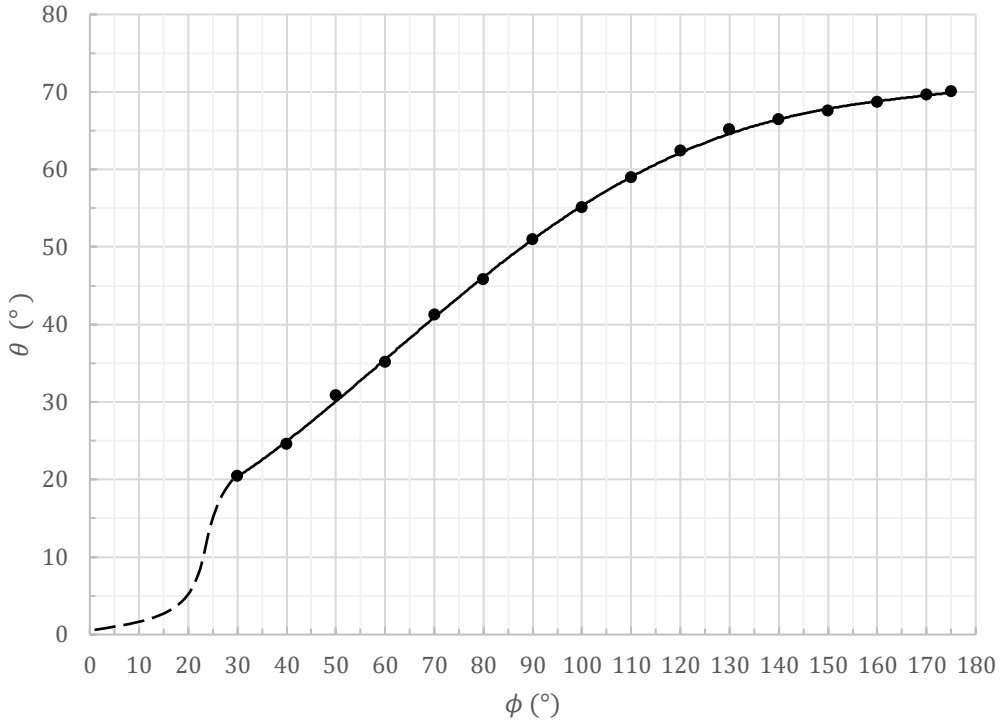

Results

Upon completion of the process of calculating the final altitude upon arrival at the landing location (if possible) and identification of the optimum bank angle for each scenario, the data was compiled and in three plots corresponding to each of the three GR values as presented in Figures 14, 15, and 16.

Figure 14
Optimum Glide Angles for $GR = 8$

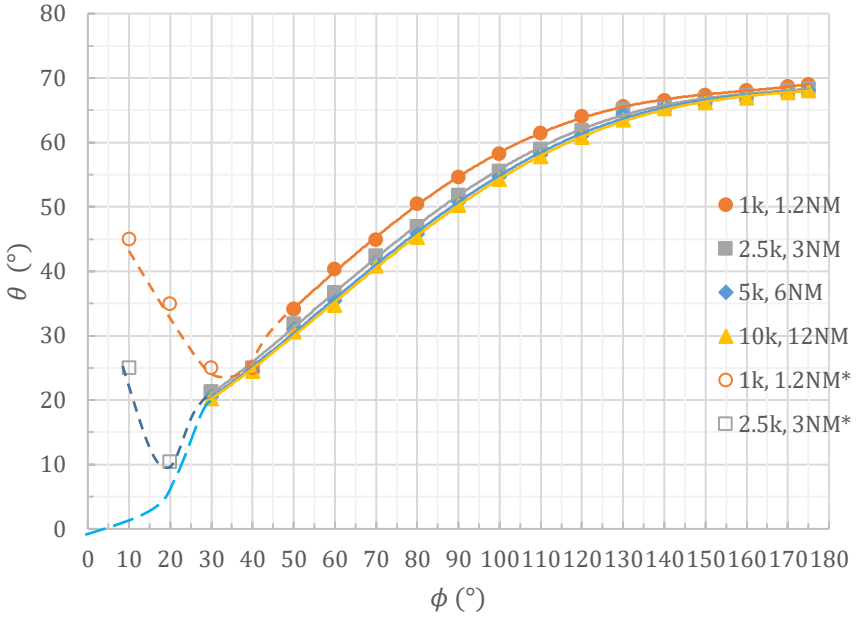

Figure 15
Optimum Glide Angles for $GR = 10$

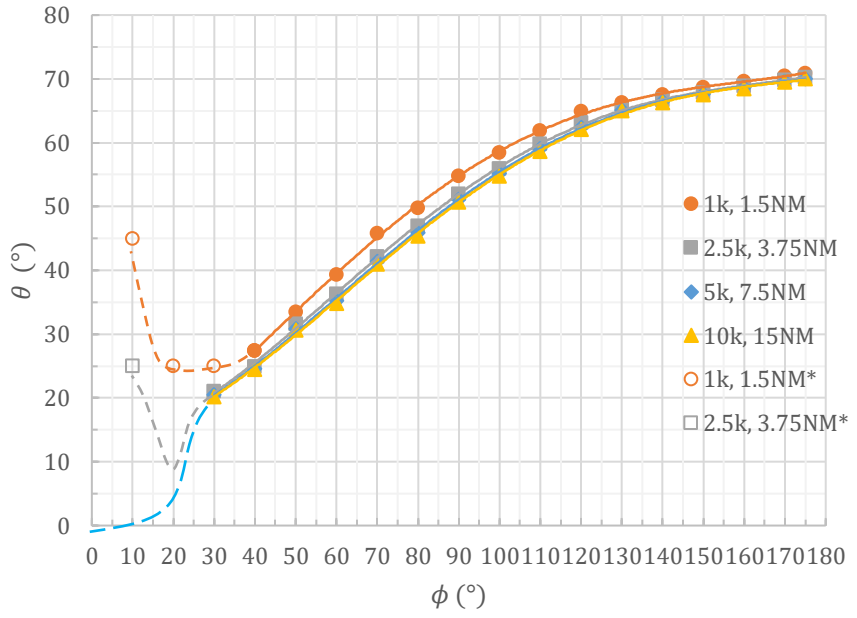

Figure 16
Optimum Glide Angles for $GR = 12$

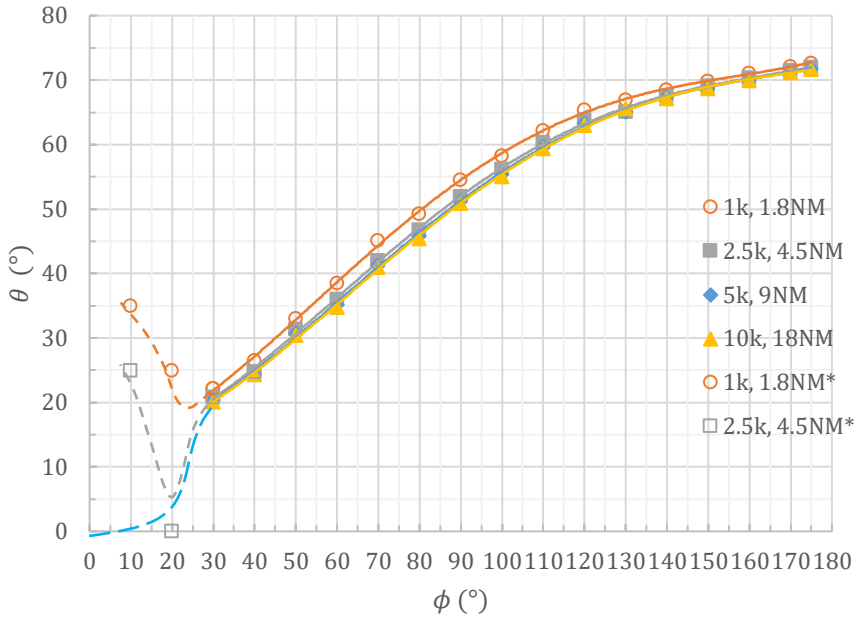

The data clearly shows that the optimum bank angle (θ) resulting in the least altitude lost in a power-off glide is a strong function of the bearing to the landing location (ϕ) and a weaker function of the airplane's GR and its altitude at the beginning of the glide (h).

For all three GRs, the optimum θ increases as ϕ increases for $\phi \geq 35°$. Although the curves are highly nonlinear, in this range of ϕ, two distinguishable regions appear that can be linearly approximated. Upon visual inspection, the domain of $35° \leq \phi < 120°$ exhibits a nearly linear relationship. Above $120°$ the curves exhibit another nearly linear relationship, albeit with a lower slope. In the domain $35° \leq \phi < 120°$, the weaker functions of altitude and GR can be seen. For all GRs tested, glides from the lowest calculated altitude have up to a $5°$ higher optimum θ when compared to the glides from higher altitudes, and for glides from the same altitude, as the airplane's GR increased, so to did the optimum θ. This relationship was mostly limited to $\phi \geq 120°$ where the difference between optimum θ from the smallest to the largest GR was approximately $5°$. Using the aggregated data for glides from $1{,}000\ ft$, (arguably the most critical altitude tested) the linear relationship for $35° \leq \phi < 120°$ was identified and is presented in Equation 29.

$$\theta \cong 0.5\phi + 10° \tag{29}$$

Glides from higher altitudes require a slight modification of Equation 29 to account for the effect of altitude. Equation 30 approximates the effects of altitude (at least for the altitudes used in these calculations) on the optimum θ, where h_k is the airplane's altitude at the beginning of the glide in thousands of feet.

$$\theta \cong 0.5\phi + \frac{5°}{h_k} + 5° \tag{30}$$

The linear relationship for $\phi \geq 120°$ was also identified using the aggregated data for glides from $1{,}000\ ft$ and is presented in Equation 31.

$$\theta \cong 0.1\phi + 52° \tag{31}$$

The altitude functionality in this domain is much weaker than that in the previous domain and is approximated in Equation 32.

$$\theta \cong 0.1\phi + \frac{1°}{h_k} + 51° \tag{32}$$

The GR functionality in this domain is slightly more prominent than was demonstrated at lower values of ϕ. This addition is approximated using Equation 33.

$$\theta \cong 0.1\phi + \frac{1°}{h_k} + \left(\frac{GR-8}{2}\right)° + 51° \tag{33}$$

An example glide calculation using Equations 30 and 33 is as follows. Suppose the airplane being flown has a published GR of 10. Equation 30 remains unchanged, but Equation 33 is updated as shown in Equation 34.

$$\theta \cong 0.1\phi + \frac{1°}{h_k} + \left(\frac{10-8}{2}\right)° + 51° = 0.1\phi + \frac{1°}{h_k} + 52° \tag{34}$$

Adjustment of Equation 33 to Equation 34 could take place well before the flight begins since the GR is a published value for the airplane. At the time of an engine failure, the closest/best landing location is found to be on a bearing of 90° (either to the left or to the right) from the airplane's heading. This means that Equation 30 should be used. If the airplane is at $2{,}500\ ft\ AGL$, the calculation of the optimum bank angle is shown in Equation 35.

$$\theta \cong 0.5(90°) + \frac{5°}{2.5} + 5° = 52° \tag{35}$$

The regions of data in the domain for $\phi < 35°$, the optimum bank angle exhibits an inverse functionality with ϕ and is much more sensitive to altitude and GR. For altitudes up to $2{,}500\ ft\ AGL$ for all GRs, there is a value of ϕ below which optimum θ increases as ϕ decreases. As an example, the $2{,}500\ ft\ AGL$ curve on the $GR = 8$ graph (Figure 14) shows a minimum θ of 25° for $\phi = 35°$, below which the optimum θ increases to 45° for the lowest calculate bearing, $\phi = 10°$. All of the curves for glides at or below $2{,}500\ ft\ AGL$ exhibit the same tendency, with the bearing associated with the minimum bank able decreasing as both altitude and GR increase. At $\phi = 10°$ the $GR = 8$ and $GR = 10$ data shows an optimum θ of 45°, while the $GR = 12$ data shows an optimum θ of only 35°. At the next altitude for $\phi = 10°$, all GRs have an optimum θ of 25°. The highest two altitudes, for which calculations were made, have optimum θs that is less than 10° at $\phi = 10°$. Given the nature of the method of identifying the optimum θ presented in a previous section, no optimum value could be identified. The blue dashed curves in Figures 14-16 extending from the higher altitudes curves is the author's estimated curve fit taking into consideration 1) the shape of the lower altitudes' curves and 2) the fact that no bank angle is necessary for a landing location on a bearing of 0° (the origin). No

simple functional relationship is obvious from the data in the domain of $\phi < 35°$, so a different view of the data is necessary.

Figures 14-16 represent the optimum values of θ that will minimize the altitude lost for a glide on any bearing to a landing location (ϕ); however, the curves do not make clear whether or not glides using the optimum values of θ will result in a positive altitude at the landing location. The glides might not be possible. Tables 4, 5, and 6 present the optimum values of θ along with whether or not the glide would be possible $(h_f \geq 0\ ft)$ for all glides with GRs of 8, 10, and 12 respectively.

Table 4

Optimum θ with $GR = 8$

ϕ (°)	θ (°, $1k$, $1.2NM$)	θ (°, $2.5k$, $3NM$)	θ (°, $5k$, $6NM$)	θ (°, $10k$, $12NM$)
10	45.0	25.0	<10	<10
20	35.0	10.4	<10	<10
30	25.0	21.3	20.6	20.3
40	25.0	25.0	24.7	24.5
50	34.1	31.9	31.0	30.6
60	40.3	36.7	35.5	34.8
70	44.9	42.4	41.4	40.9
80	50.5	47.0	45.8	45.3
90	54.6	51.8	50.8	50.3
100	58.3	55.6	54.7	54.3
110	61.4	59.0	58.2	57.8
120	64.1	61.9	61.2	60.8
130	65.6	65.1	64.5	63.5
140	66.5	65.7	65.5	65.3
150	67.3	66.6	66.3	66.2
160	68.1	67.4	67.1	67.0
170	68.7	68.1	67.9	67.8
175	69.0	68.4	68.2	68.1

Note. Shaded values of θ indicate that the glide resulted in only negative altitudes; therefore, it was not possible. Blue values of θ indicate that the glide was possible; however, at least the lowest, if not several of the lowest, values of θ resulted in failed glides. Green values of θ indicate that the glide was possible; however, at least the lowest θ, if not several of the lowest, and at least the highest values of θ, if not several of the highest, resulted in failed glides. Black values of θ indicate that the glide was possible for all θ (10° – 80°).

Table 5

Optimum θ with $GR = 10$

ϕ (°)	θ (°, $1k$, $1.5NM$)	θ (°, $2.5k$, $3.75NM$)	θ (°, $5k$, $7.5NM$)	θ (°, $10k$, $15NM$)
10	45.0	25.0	<10	<10
20	25.0	<10	<10	<10
30	25.0	21.0	20.5	20.2
40	27.4	24.9	24.6	24.5
50	33.5	31.6	30.9	30.6
60	39.3	36.3	35.3	34.8
70	45.8	42.1	41.4	41.0
80	49.8	46.9	45.9	45.4

90	54.8	51.9	51.1	50.7
100	58.4	56.0	55.2	54.8
110	61.9	59.8	59.1	58.7
120	64.9	63.1	62.5	62.1
130	66.3	65.1	65.1	65.0
140	67.5	66.7	66.4	66.3
150	68.7	67.9	67.6	67.5
160	69.6	68.9	68.7	68.5
170	70.5	69.8	69.6	69.5
175	70.9	70.3	70.1	70.0

Note. Shaded values of θ indicate that the glide resulted in only negative altitudes; therefore, it was not possible. Blue values of θ indicate that the glide was possible; however, at least the lowest, if not several of the lowest, values of θ resulted in failed glides. Green values of θ indicate that the glide was possible; however, at least the lowest θ, if not several of the lowest, and at least the highest values of θ, if not several of the highest, resulted in failed glides. Black values of θ indicate that the glide was possible for all θ $(10° - 80°)$.

Table 6

Optimum θ with $GR = 12$

ϕ (°)	θ $(°, 1k, 1.8NM)$	θ $(°, 2.5k, 4.5NM)$	θ $(°, 5k, 9NM)$	θ $(°, 10k, 18NM)$
10	35.0	25.00	<10	<10
20	25.0	<10	<10	<10
30	22.2	20.8	20.4	20.1
40	26.5	24.8	24.5	24.4
50	33.0	31.4	30.8	30.5
60	38.5	36	35.2	34.8
70	45.2	42	41.3	41.0
80	49.2	46.8	45.9	45.5
90	54.5	52	51.3	50.9
100	58.3	56.2	55.5	55.1
110	62.2	60.3	59.7	59.4
120	65.4	63.9	63.3	63.0
130	66.9	65.1	65.1	65.6
140	68.5	67.6	67.4	67.2
150	69.9	69.1	68.8	68.7
160	71.1	70.4	70.1	70.0
170	72.2	71.5	71.3	71.2
175	72.7	72	71.8	71.7

Note. Shaded values of θ indicate that the glide resulted in only negative altitudes; therefore, it was not possible. Blue values of θ indicate that the glide was possible; however, at least the lowest, if not several of the lowest, values of θ resulted in failed glides. Green values of θ indicate that the glide was possible; however, at least the lowest θ, if not several of the lowest, and at least the highest values of θ, if not several of the highest, resulted in failed glides. Black values of θ indicate that the glide was possible for all θ $(10° - 80°)$.

Values in the table are coded using shading and text color. Shaded cells indicate that glides from those altitudes and to those bearings are not possible. Blue text indicates that the glides are possible; however, they are only possible when using higher bank angles. Turning with at least the lowest bank angle won't allow the airplane to reach its destination. Green text indicates that the glides are possible but not at the lowest or the highest bank angles. It indicates that several of the low and high bank angles will result in unsuccessful glides. Black text indicates that glides are possible from those altitudes and to those bearings and that they are possible throughout the range of tested bank angles $(10° - 80°)$.

From inspection of the tables, an obvious and expected result is that increased GRs provide more gliding options. Another obvious result is that within one $GR's$ data (i.e., Table 4), higher altitudes provide more gliding options. The data for glides from altitudes up to $2{,}500\ ft$ for all GRs shows that the lowest bank angles should be avoided for glides to destinations at low bearings, and glides to the locations at higher bearings (if possible) are only possible when avoiding the lowest and the highest bank angles.

Recall that Equation 30 applies to $35° \leq \phi < 120°$, and Equation 33 applies to $\phi \geq 120°$. The first three rows of Tables 4-6 are for $\phi < 35°$. The majority of glides described by these rows are optimized at extremely low bank angles but will still be possible at high bank angles (black text). An approximate functional relationship in this domain of low bearings is presented in Equation 36.

$$\theta \cong \phi - 10° \tag{36}$$

This equation only applies to glides from altitudes at or above $2{,}500\ ft$ and for bearings of no less than $20°$. The critical glides are from the lower altitudes and bearings, located in the upper left corner of the tables. These glides aren't possible when using the lowest bank angles and are optimized at bank angles of up to $45°$. The reason for this is that the lowest bank angles have high turn radii and will not allow an airplane to reach an intercept path to the landing location. A turn must be tighter to achieve an intercept path when the landing location is so close. These findings are in agreement with those of Rogers (1995) for low-altitude gliding turns. Equation 37 presents the criteria that enable a turn to an intercept course to be possible, where r is the turn's radius from Equation 15 and d is the airplane's distance from the landing location.

$$r \leq \frac{d}{2} \tag{37}$$

The most critical of the scenarios tested was a glide from $1{,}000\ ft$ to a landing destination on a bearing of $10°$ with an GR of 10 or less. These glides have an optimum bank angle of $45°$ and are not even possible at bank angles of less than $40°$ due to the inability of lower banked turns to achieve an intercept course. No simple functional relationship for optimum bank angle was developed for gliding turns to locations within the critical domains shown in the tables due to the highly nonlinear relationship between θ and r in Equation 15; however, a $45°$ banked turn will not only enable a successful glide in the critical domains, it will also work for glides from higher altitudes in this domain for any of the tested GRs.

Conclusions

It is common (and required) knowledge among pilots that in order to maximize power-off glide distance an airplane must be flown at its v_G. It seems to be less common (and not required) knowledge among pilots that an airplane's v_G is a function of its weight and that the published v_G only applies to the airplane at its $MTOW$. Adjusting a published v_G using Equation 11 is necessary to ensure that the highest GR $(a.k.a.\ \ L/D)$, and hence the maximum range, is achieved.

Even less known among pilots is that when a turn is required to make it to a safe landing location in a power-off glide, the bank angle used in the gliding turn can be optimized for maximum glide performance. It was shown that for glides requiring a turn to a landing location with a bearing greater than or equal to $120°$ from the airplane's heading, Equation 33 (reproduced here) provides a simplified approximation to the turn's optimum bank angle.

$$\theta \cong 0.1\phi + \frac{1^\circ}{h_k} + \left(\frac{GR-8}{2}\right)^\circ + 51^\circ \tag{33}$$

The equation is simplified using an airplane's GR, after which the only inputs are the bearing to the landing location and the airplane's AGL altitude in thousands of feet. Due to the simple nature of Equation 33, it is perfectly suitable for mental math. As an example, an airplane with a GR or 10, which can be incorporated into the equation beforehand, loses its engine at $3{,}000\ ft$ with the best landing location on a $150°$ bearing. The simple nature of Equation 33 (e.g., multiplying by 0.1 only requires that the bearing's decimal point be moved once to the left) quickly reveals a $67°$ optimal bank angle for the turn. This example exposes the issue of bank angles exceeding $60°$. CFR 14, Part 23.3 (2011) prohibits normal category airplanes from being flown at bank angles that exceed $60°$; however, CFR 14 Part 91.3 (1989) allows a pilot in command to deviate from other regulations in order to deal with an emergency. In-flight engine failures are definitely emergencies. If turning to a safe landing destination during an engine-out glide is best performed with a bank angle higher than $60°$, regulations won't prevent it. Concerns associated with high bank angle turns are related to pilot skill while operating at unusual attitudes and high load factors. Pilot skills will be left to training and experience. The normal category load factor limit is an issue at bank angles above $74°$ for constant altitude turns. This is not an issue for gliding turns, since 1) load factors are lower when not maintaining altitude and 2) all of the optimum bank angles were less than $72°$.

For gliding turns to landing locations with bearings between $35°$ and $120°$, Equation 30 (reproduced here) provides an even simpler (independent of GR) approximation to the turn's optimum bank angle.

$$\theta \cong 0.5\phi + \frac{5^\circ}{h_k} + 5^\circ \tag{30}$$

As an example, an airplane loses its engine at $3{,}000\ ft$ with the best landing location on a $60°$ bearing. The simple nature of Equation 30 quickly reveals a $37°$ optimal bank angle for the turn.

For gliding turns to landing locations with bearings of less than $35°$, the optimum bank angle is approximated by Equation 36; however, the equation is limited to certain bearings and altitudes. Due to the critical low-bearing, low-altitude domain that has high optimum bank angles, all gliding turns to landing locations with bearings of less than $35°$ would be successful, albeit not optimized, when conducted with a bank angle of $45°$.

Recommendations

Using the information presented in this paper, the majority of which is the result of original research into optimum bank angles to be used during power-off glides, the author makes the following recommendations.

1. Digital avionics and flight management systems should incorporate real-time glide performance information to include:
    a. Displays of weight-corrected v_G using 1) an initial weight entered at the beginning of a flight by the pilot and 2) fuel flow measurements,
    b. Real-time glide range corrected for range losses due to turns in all directions using optimal bank angles, and
    c. The optimum bank angle to use during a power-off glide to an intercept course for a suitable landing location 1) that has been identified and selected by the pilot or 2) that has been selected by the system and presented to the pilot.

2. Pilot education/instruction and reference materials (i.e., course content, handbooks, and manuals) should present more detailed power-off glide performance information including:
    a. Use of Equation 11 for weight-correcting v_G along with recommending the options of 1) calculating the minimum possible v_G corresponding to the airplane's lowest possible weight for interpolation in-flight or 2) creating a graph similar to Figure 4 for quick reference in flight and
    b. Use of rule-of-thumb equations/guides for calculating optimum bank angle to include 1) Equation 33 for glides to bearings above $120°$, 2) Equation 30 for glides to bearings between $35°$ and $120°$, and 3) $45°$ for glides to bearings less than $35°$.

3. Flight training should include the practice of in-flight power-off glide scenarios that include 1) the identification of safe landing locations within glide range, 2) the calculation of optimum bank angles for glides to different bearings, and 3) turns to intercept courses.

References

Adler, A., Bar-Gill, A., & Shimkin, N. (2012). Optimal Flight Paths for Engine-Out Emergency Landing. *2012 24th Chinese Control and Decision Conference (CCDC)*, (pp. 2908-2915). Taiyuan.

Airplane Categories. (2011). 14 Code of Federal Regulations, Part 23.3.

Airplane Flying Handbook. (2021). Oklahoma City: Federal Aviation Administration.

Asselin, M. (1997). *An Introduction to Aircraft Performance.* Reston: American Institute of Aeronautics and Astronautics, Inc.

Atkins, E. M., Portillo, I. A., & Strube, M. J. (2006). Emergency Flight Planning Applied to Total Loss of Thrust. *Journal of Aircraft, 43*(4), 1205-1216.

Beech Bonanza A36 Pilot's Operating Handbook and FAA Approved Airplane Flight Manual. (2006). Wichita: Raytheon Aircraft Company.

Chitsaz, H., & LaValle, S. M. (2007). Time-Optimal Paths for a Dubins Airplane. *2007 46th IEEE Conference on Decision and Control*, (pp. 2379-2384). New Orleans.

Di Donato, P. F., & Atkins, E. M. (2016). Optimizing Steady Turns for Gliding Trajectories. *Journal of Guidance, Control, and Dynamics, 39*(12), 2627-2637.

(2011). *Flight Test Guide for Certification of Part 23 Airplanes.* Oklahoma City: Federal Aviation Administration.

Glide: Single-Engine Airplanes. (1996). 14 Code of Federal Regulations, Part 23.71.

Hurt, H. H. (1965). *Aerodynamics for Naval Aviators.* Los Angeles: Naval Air Systems Command.

Jacobs, E. N., Ward, K. E., & Pinkerton, R. M. (1933). *The Characteristics of 78 Related Airfoil Sections from Tests in the Variable-Density Wind Tunnel.* National Advisory Committee for Aeronautics.

Meuleau, N., Plaunt, C., Smith, D. E., & Smith, T. (2009). An Emergency Landing Planner for Damaged Aircraft. *Proceedings of the Twenty-First Innovative Applications of Artificial Intelligence Conference.* Pasadena.

Ranjan, P., Collazo Garcia, A. R., Chen, K. J., James, K. A., & Ansell, P. J. (2021). Flight Trajectory Optimization of Sailplane After Rope Break. *Journal of Aircraft, 58*(6), 1229-1241.

Responsibility and Authority of the Pilot in Command. (1989). 14 Code of Federal Regulations, Part 91.3

Rogers, D. F. (1995). The Possible 'Impossible' Turn. *Journal of Aircraft, 32*, 392-397.

Segal, D., Bar-Gill, A., & Shimkin, N. (2019). Max-Range Glides in Engine Cutoff Emergencies Under Severe Wind. *Journal of Guidance, Control, and Dynamics, 42*(8), 1822-1835.

Stephan, J., & Fichter, W. (2016). Fast Generation of Landing Paths for Fixed-Wing Aircraft with Thrust Failure. *AIAA Guidance, Navigation, and Control Conference.* San Diego.

A publication of the University Aviation Association, © 2023